
Theoretical Physics

# Quantum Random Walks with Perturbing Potential Barriers

André Schwalbe Lehtihet
lehtihet@kth.se
Oscar Lindvall Bulancea
oscarlb@kth.se
SA114X Degree Project in Engineering Physics, First Level
Department of Theoretical Physics
Royal Institute of Technology (KTH)
Supervisor: Mats Wallin

May 20, 2017

**Abstract**

With a recent interest in quantum computers, the properties of quantum mechanical counterparts to classical algorithms have been studied in the hope of providing efficient algorithms for quantum computers. Because of the success of classical random walks in providing good algorithms on classical computers, attention has been turned to quantum random walks, since they may similarly be used to construct efficient probabilistic algorithms on quantum computers. In this thesis we examine properties of the quantum walk on the line, in particular the standard deviation and the shape of the probability distribution, and the effect of potentials perturbing the walk. We model these potentials as rectangular barriers between the walker's positions and introduce a probability of the walker failing to perform the step procedure, similar to that of Wong in Ref. [14]. We find that a potential localized around the starting position leads to an increased standard deviation and makes the walk increasingly ballistic. We also find that uniformly distributed random potentials have the general effect of localizing the distribution, similar to that of Anderson localization.

**Sammanfattning**

I och med ett ökat intresse för kvantdatorer har egenskaper av kvantmekaniska motsvarigheter till klassiska algoritmer studerats i hopp om att ta fram effektiva algoritmer för kvantdatorer. Eftersom klassiska slumpvandringar med goda resultat använts för att implementera algoritmer på klassiska datorer har uppmärksamhet riktats mot kvantmekaniska slumpvandringar, då de på liknande sätt skulle kunna användas för att konstruera effektiva probabilistiska algoritmer för kvantdatorer. I det här examensarbetet undersöker vi några av kvantvandringens egenskaper på linjen, särskilt standardavvikelsen och sannolikhetsfördelningens form, samt hur godtyckliga potentialer påverkar vandringen. Vi modellerar dessa potentialer som rektangulära barriärer mellan vandrarens positioner and introducerar en sannolikhet att vandrarens steg inte genomförs, liknande hur Wong gjort i Ref. [14]. Vi finner att en potential lokaliserad runtom vandrarens startposition resulterar i en högre standardavvikelse och gör gången mer ballistisk. Vi finner även att en likformigt fördelad slumpmässig potential har den allmänna effekten att lokalisera fördelningen, liknande Andersonlokalisering.

# Contents

# Chapter 1

# Introduction

The development of quantum computers and the methods of quantum computation is an area of research that has received a large amount of attention in recent years. While the development of quantum computers is still in its infancy, it is actively progressing, and if it reaches the point of practical use, the algorithms already developed promise significant increase in problem solving capabilities. Not only could quantum computers provide better algorithms, we would also retain the capabilities of the classical computer since, as explained by Kempe [1], any algorithm implemented on a classical computer can be emulated on a quantum computer, providing the same efficiency. Out of the algorithms already developed, Shor's algorithm for factoring numbers is notable as it is capable of factoring a number into its prime factors in polynomial time, something no known algorithm on a classical computer has achieved [2]. If run on a sufficiently powerful quantum computer, it could be capable of breaking most public-key encryptions. Another algorithm showing promise is Grover's algorithm for searching an unordered data structure. If correctly implemented, it would be able to find an element in an unordered data structure of size $N$ with $O(\sqrt{N})$ operations, as opposed to the $O(N)$ limit of any classical computer [3]. The search for quantum algorithms such as these often start by looking at and modifying classical algorithms and techniques known to be useful. Stochastic algorithms are of particular interest, because of the probabilistic nature of quantum mechanics. In particular, attention has been given to the classical random walk, being the foundation of many classical algorithms. In this thesis, we look at the classical random walk and its quantum counterpart, and we start with a basic introduction to both of them.

## 1.1 Classical Random Walks

The classical random walk is an abstract procedure in which we let some object, generally referred to as a walker, traverse some structure non-deterministically. Whether the walker traverses the structure at discrete time intervals, or at any given time with some probability, classifies the walk type as discrete or continuous, respectively.

A very simple example would be the unbiased discrete random walk on the discrete infinite line, jokingly referred to as the "drunkard's walk", in which a walker starting out at some start position $i$, "walks" the line by either going right to position $i + 1$ with probability $\frac{1}{2}$ or left to $i - 1$ with probability $\frac{1}{2}$, at discrete time intervals. The action of deciding the direction to go is often referred to as "flipping a coin".

Of course one could generalize the walk by instead letting the walker traverse an arbitrary graph, instead formulating the procedure as the particle starting at some vertex, traversing the graph by walking along one of the available edges with some probability at each step.

The classical random walk is applicable in solving a number of problems and can be used effectively in a multitude of computer algorithms. Two examples, given by Kempe [1], are the $k$-SAT problem and the S-T connectivity problem. The $k$-SAT problem is formulated as follows: Given a set of $n$ logical clauses $C_1, C_2, \ldots, C_n$ of length $k$, taking $m$ boolean variables $X_1, X_2, \ldots, X_m \in \{\text{False, True}\}$ as input, the goal is to find an assignment to the variables such that all the clauses are satisfied simultaneously. A concrete example would be the following instance of a 2-SAT problem, $\Phi(X_1, X_2, X_3) = (\neg X_1 \vee X_2) \wedge (X_1 \wedge X_3) \wedge (X_2 \vee X_3)$ which has a trivial solution $X_1 = X_2 = X_3 = \text{True}$. The $k$-SAT problem can be shown to be NP-complete, which means it is among the problems not known to have an efficient solution, but having an efficient solution would mean having an efficient solution to all NP problems. The algorithm making up the most efficient solution for $k$-SAT, known today, is in fact a more sophisticated version of the random walk [4]. The S-T connectivity problem is the problem of checking if there is a path in a graph that connects to nodes $S$ and $T$. The problem can be solved by any basic graph search algorithm, but searching by random walk drastically decreases memory usage and can be more efficient for particularly large and dense graphs [1].

## 1.2 Quantum Walks

In the quantum case, the walker has the property of not having a well-defined position. As the walk will be performed by a quantum particle of some sort, or be simulated by a qubit in a quantum computer, the walk induces a *superposition* of different positions of the walker that only gives a definite position once measured. This is the key property that distinguishes the quantum from the classical random walk and what induces radically new behavior and properties on the walk. Another difference is that the coin flip of the classical walk is replaced by a deterministic process which sets up the walker to walk in several directions simultaneously. We will go into further detail on how the quantum walk works in later sections as the process is more involved than the classical random walk.

As already mentioned, there is hope that this kind of quantum random walk could similarly be used in algorithms, with a speed-up compared to the classical case, implemented on a quantum computer. There are cases where the quantum walk can give an exponential speed-up to algorithms, compared to the classical random walk, for example random walk search on the hypercube explained in Ref. [5]. The Grover algorithm mentioned above can also be implemented as a quantum random walk.

Note that while random walks can be defined on any graph structure in both the classical and quantum case, we will in this thesis concern ourselves only with walks on a one-dimensional grid $\mathbb{Z}$.

# Chapter 2

# Background Material

The start of this chapter reviews some basic properties of the one-dimensional, unbiased classical random walk. For the rest of the study, we will only examine discrete walks, as they are the focus of many experiments implementing the quantum walk. Perhaps the first question that comes to mind regarding the walk is how the probability distribution of finding the walker at position $x$ looks like after a number of steps $t$.

## 2.1 Basic Properties of the Classical Random Walk

For the classical walk, the probability distribution can be found analytically by combinatorial methods, explained in Ref. [6]. The distribution of an unbiased classical walk on the line, having equal probability of going to the right or left at each step, with starting position $x = 0$, is given by

$$p(x,t) = \frac{1}{2^t}\binom{t}{\frac{t+x}{2}}, \tag{2.1}$$

describing the probability of being at position $x$ after $t$ steps, valid for $|x| \leq t$ and where $t+x$ is even. If $t+x$ is odd, the probability of the walker being at position $x$ is zero, since the walker can never be at an odd-numbered position after an even amount of steps and vice versa. For a given $t$, this defines a binomial distribution and is shown for $t = 100$ in Fig. 2.1. The standard deviation of such a probability distribution can be shown [6] to be proportional to the square root of the number of steps taken, $\sigma \sim \sqrt{t}$. The standard deviation is an important property of the walk as it characterizes the propagation speed of the walker. Note that the probability distribution, as seen in Fig. 2.1, has its only maximum at the starting position of the walk. Both this property and how the standard deviation of the walk changes with $t$, defines what is called diffusive behaviour, and as we will see, is in stark contrast to the quantum walk.

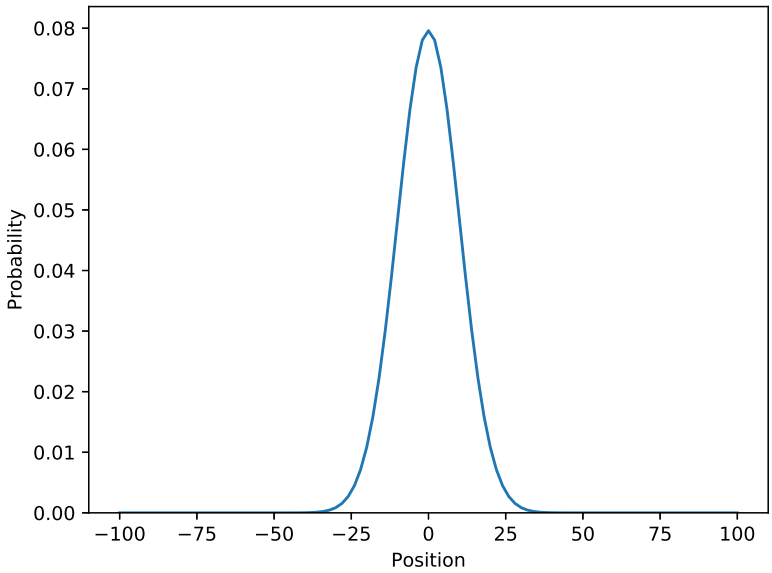


Figure 2.1: Probability distribution of the classical random walk, starting at position $x = 0$, after 100 steps. Note that we have not included the probability at odd-numbered positions where the probability is zero.

## 2.2 Definition of Quantum Walks

It is not immediately clear precisely what a quantum version of the classical random walk should be, but we can insist on some of its properties. For instance the definite position of the walker must be replaced in some manner by a state vector $|\psi\rangle$ in some Hilbert space $\mathcal{H}$ which encodes the probabilities of finding the walker on the positions of the grid. But will this generalization work on its own? Assuming it will, let that Hilbert space $\mathcal{H}_p$ be spanned by the orthonormal basis vectors $\{|i\rangle : i \in \mathbb{Z}\}$. If we perform a step in the walk, under these assumptions, we must for a walker localized in a state $\psi = |k\rangle$, where $k$ is an integer, end up in some superposition $U|k\rangle = \alpha|k-1\rangle + \beta|k+1\rangle$, where $\alpha$ and $\beta$ are complex constants and $|\alpha|^2 + |\beta|^2 = 1$ and $U$ is the step-operator, which performs a step in the walk. If we want an analogue to the classical walk, we want to be able to construct a walk that is translationally invariant, i.e. independent of start position and that works the same everywhere. In that case, the constants $\alpha$ and $\beta$ must be independent of the position $k$. The step operator $U$ must also be unitary, i.e. preserving the norm $\langle\psi|\psi\rangle = 1$ of the state or, equivalently, fulfilling $U^\dagger U = I$, if we are to keep our probability interpretation of $|\psi|^2$. Consider then the states $|\psi_{-1}\rangle := U|x-1\rangle = \alpha|x-2\rangle + \beta|x\rangle$ and $|\psi_1\rangle := U|x+1\rangle = \alpha|x\rangle + \beta|x+2\rangle$. The basis is orthonormal, which gives $\langle\psi_{-1}|\psi_1\rangle = \langle x-1|U^\dagger U|x+1\rangle = \langle x-1|x+1\rangle = 0$ but we also have $\langle\psi_{-1}|\psi_1\rangle = \alpha\beta^*$ which is zero only for $\alpha$ or $\beta$ zero, which would make for an incredibly dull walk.

We see that the quantum walk cannot be modeled quite so easily. Instead of choosing an operator and vector space as above, the common approach is to expand our Hilbert space with another, two-dimensional, space $\mathcal{H}_c$, the so called coin space, spanned by the orthonormal basis vectors $\{|\uparrow\rangle, |\downarrow\rangle\}$. Our new Hilbert space is now $\mathcal{H} = \mathcal{H}_c \bigotimes \mathcal{H}_p$ where $\mathcal{H}_p$ is the same as above and we have made use of the tensor product construction of a new vector space from two other ones. The vectors in this new vector space consists of products of the vectors from the spaces $\mathcal{H}_c$ and $\mathcal{H}_p$. For example, $|\uparrow\rangle \otimes |0\rangle \in \mathcal{H}$ is a basis vector of $\mathcal{H}$, which is spanned by the product of the basis vectors from the spaces $\mathcal{H}_c$ and $\mathcal{H}_p$. The basis vectors are thus $|\uparrow\rangle \otimes |i\rangle$ and $|\downarrow\rangle \otimes |i\rangle$, $i \in \mathbb{Z}$. We refer to Ref. [7] for details on the tensor product between vector spaces. The coin space $\mathcal{H}_c$ is used to give the walker a direction before performing the actual step, but will also allow the walker to be in a superposition of different directions. At each iteration of the walk, the coin space will be changed by a unitary transformation acting analogous to the coin flip of the classical walk.

A very common choice of this transformation is the Hadamard operator, or Hadamard coin, defined as

$$H : \begin{cases} |\uparrow\rangle \xrightarrow{H} \dfrac{|\uparrow\rangle + |\downarrow\rangle}{\sqrt{2}} \\ |\downarrow\rangle \xrightarrow{H} \dfrac{|\uparrow\rangle - |\downarrow\rangle}{\sqrt{2}} \end{cases}, \tag{2.2}$$

which corresponds to an unbiased walk, since a walker initially in a state $|\uparrow\rangle$ (or $|\downarrow\rangle$) is then mapped to an equal superposition of the different coin states. If we identify the coin states with vectors such that $|\uparrow\rangle = \begin{pmatrix} 1 \\ 0 \end{pmatrix}$ and $|\downarrow\rangle = \begin{pmatrix} 0 \\ 1 \end{pmatrix}$, the Hadamard coin can be written in matrix form as

$$H = \frac{1}{\sqrt{2}} \begin{bmatrix} 1 & 1 \\ 1 & -1 \end{bmatrix}.$$

This is essentially the only interesting coin for an unbiased walk in one dimension. There are other coins capable of representing an unbiased walk, but they do not present any new kind of distribution to the walk. All distributions for an unbiased walk can be obtained with the Hadamard coin and suitable initial state, as is remarked in Ref. [8].

The walk will then proceed as follows:
The walker is initialized in some state $|\psi\rangle = (\alpha |\uparrow\rangle + \beta |\downarrow\rangle) \otimes |x\rangle$. The direction, i.e. the coin state, of the walker is acted on by a coin-flip transformation $C$, in our case $C = H$, whereby a conditional shift $S$ takes place, taking the part of the walker which is in the $|\uparrow\rangle$ direction to the right and the $|\downarrow\rangle$ part to the left. This shift operator is in most cases defined as

$$S = |\uparrow\rangle \langle\uparrow| \otimes \sum_{i=-\infty}^{\infty} |i+1\rangle \langle i| + |\downarrow\rangle \langle\downarrow| \otimes \sum_{i=-\infty}^{\infty} |i-1\rangle \langle i|,$$

but other definitions of the shift operator will be considered later in this thesis. $S$ then takes basis vectors $|\uparrow\rangle \otimes |i\rangle$ to $|\uparrow\rangle \otimes |i+1\rangle$ and $|\downarrow\rangle \otimes |i\rangle$ to $|\downarrow\rangle \otimes |i-1\rangle$. Note that all operators used in this thesis will be linear and so it is sufficient to specify how they act on their respective basis vectors to define how they act on any vector.

The total evolution operator of the walker is then given by

$$U = S(C \otimes I_p), \tag{2.3}$$

where $C$ is the coin flip operator and $I_p$ is the identity operator acting on the position space $\mathcal{H}_p$. A walker in the initial state $|\psi_0\rangle$ is then after $T \in \mathbb{Z}^+$ steps in the state $|\psi_T\rangle = U^T |\psi_0\rangle$. Below, we show an illustrative example of a three-step walk with the Hadamard coin, for the initial state $|\psi_0\rangle = |\uparrow\rangle \otimes |0\rangle$:

$$
\begin{aligned}
\psi_0 &\xrightarrow{C\otimes I_p} \frac{1}{\sqrt{2}}(|\uparrow\rangle + |\downarrow\rangle) \otimes |0\rangle \\
&\xrightarrow{S} \frac{1}{\sqrt{2}}(|\uparrow\rangle \otimes |1\rangle + |\downarrow\rangle \otimes |-1\rangle) = |\psi_1\rangle \\
&\xrightarrow{C\otimes I_p} \frac{1}{2}((|\uparrow\rangle + |\downarrow\rangle) \otimes |1\rangle + (|\uparrow\rangle - |\downarrow\rangle) \otimes |-1\rangle) \\
&\xrightarrow{S} \frac{1}{2}(|\uparrow\rangle \otimes |2\rangle + (|\uparrow\rangle + |\downarrow\rangle) \otimes |0\rangle - |\downarrow\rangle \otimes |-2\rangle) = |\psi_2\rangle \\
&\xrightarrow{C\otimes I_p} \frac{1}{2\sqrt{2}}((|\uparrow\rangle + |\downarrow\rangle) \otimes |2\rangle + 2\,|\uparrow\rangle \otimes |0\rangle - (|\uparrow\rangle - |\downarrow\rangle) \otimes |-2\rangle) \\
&\xrightarrow{S} \frac{1}{2\sqrt{2}}(|\uparrow\rangle \otimes |3\rangle + (2\,|\uparrow\rangle + |\downarrow\rangle) \otimes |1\rangle - |\uparrow\rangle \otimes |-1\rangle + |\downarrow\rangle \otimes |-3\rangle) = |\psi_3\rangle\,.
\end{aligned}
$$

## 2.3 Principal Differences

The most striking difference between the classical and quantum walks is the very different probability distribution of the quantum walk, caused by interference between the different walker paths. As can be seen in the example above in the third step, the probability of being found in position 1 after a position measurement is not the same as the one of being in $-1$. The distribution of the unbiased walk becomes asymmetric. The coin space has granted an extra two degrees of freedom which affect the walk and makes it dependent on the initial state configuration. This is in contrast to the classical case, where one can only choose the start position, which for unbiased walk has no effect other than translating the distribution. The resulting probability distributions of the two basic asymmetric initial states $|\psi_0\rangle = |\uparrow\rangle \otimes |0\rangle$ and $|\psi_0\rangle = |\downarrow\rangle \otimes |0\rangle$ can be found by simulating the walk and is shown in Fig. 2.2. Note that since the Hadamard coin is a real operator, the real and imaginary parts of $|\psi_0\rangle = \frac{1}{\sqrt{2}}(|\uparrow\rangle + i\,|\downarrow\rangle) \otimes |0\rangle$ never mix and so the walk from this initial state can be viewed as the mean of the walks from the two basic asymmetric initial states. This results in a symmetric walk, as is seen in Fig. 2.3, and will be used throughout the study.

Regardless of initial state, the standard deviation in the quantum case has been shown to go as $\sigma \sim t$ [6], which is referred to as ballistic propagation. Note that this is quadratically faster than the classical random walk where $\sigma \sim \sqrt{t}$.

The sources of randomness is very different in the classical and quantum walks. In the classical case the only source of randomness is the stochastic process of the coin toss. The quantum mechanical counterpart to the coin toss, the coin flip operator $C$ involves no random process, and neither does the conditional shift operator $S$. Thus the only reason that a probability distribution is induced is because of the inherent quantum nature of the walker. The quantum random walk itself is thus random only in name which is why we often refer to it simply as the quantum walk.

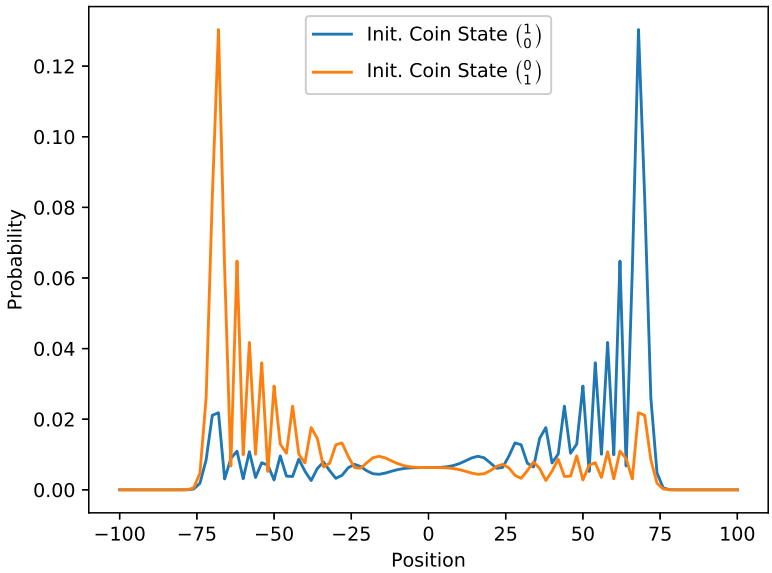


Figure 2.2: Probability distributions of the quantum walk with initial state $|\psi_0\rangle = |\uparrow\rangle \otimes |0\rangle$ and $|\psi_0\rangle = |\downarrow\rangle \otimes |0\rangle$ after 100 steps. Note that we have not included the probability at odd-numbered positions where the probability is zero.

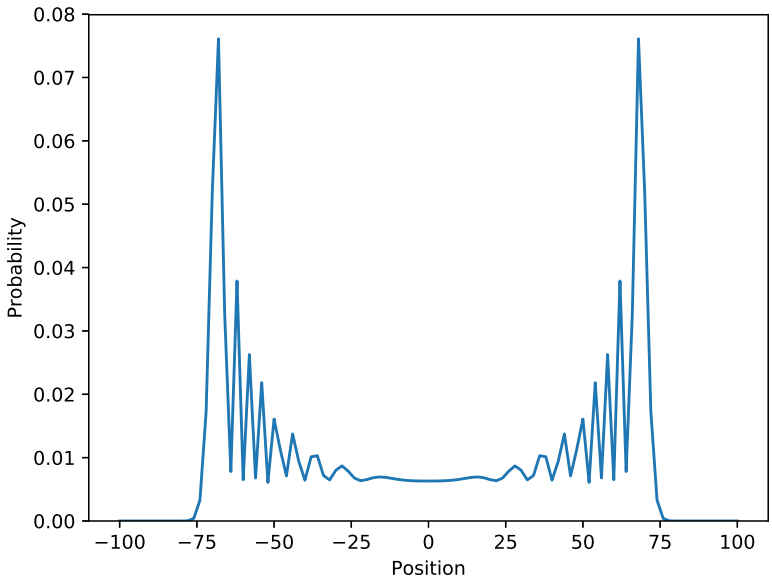


Figure 2.3: Probability distribution of the quantum walk with initial state $|\psi_0\rangle = \frac{1}{\sqrt{2}}(|\uparrow\rangle + i\,|\downarrow\rangle) \otimes |0\rangle$ after 100 steps. We have not included the probability at odd-numbered positions.

## 2.4 Physical Implementation

Quantum walks are of course not very interesting if we have no chance of actually implementing them in a real physical system. A number of ways to implement a quantum random walk have been suggested [9][10][11][12], and we will review the approach taken in Ref. [12]. There, they realize the one-dimensional discrete quantum walk with the Hadamard coin by letting the line be represented by a 1D magneto-optical lattice. The walker is a laser-cooled cesium atom which can be trapped in the potential wells of the optical lattice, thus creating a discrete position space. The coin state is then realized by preparing the atom in a hyperfine state by optical pumping, which involves fixing the total angular momentum of the atom by raising its electron energy levels through laser photon absorption. This hyperfine state is then coupled to another hyperfine state by resonant microwave radiation, to represent the opposite coin state. It is then possible to prepare the atom in the symmetric state, or apply the Hadamard operator, through a series of microwave pulses, so called $\pi/2$- and $3\pi/2$-pulses. By careful control of the optical lattice potentials, the atoms can be made to shift to nearby positions according to their hyperfine states. Although, one difference to the walk as we explained earlier is that the coin states are flipped after the shift operation.

### Difficulties With the Physical Implementation

When implementing the walk as in Ref. [12] or similar cases, there are a number of factors capable of perturbing the walk procedure. Other than errors in the experimental equipment, the most influential factor is the difficulty of preventing decoherence, i.e. keeping the walker from interfering with its surroundings, and making sure the walk proceeds as intended. Such phenomena can considerably impair the properties of the walk, such as reducing the propagation of the probability distribution, effectively reducing the standard deviation.

Given enough decoherence, for example letting the walker be measured after each step, the walker will become completely localized at every step and the quantum walk will thus be reduced to the classical walk, as is mentioned by Kempe [1]. However, it has been pointed out by Kendon and Tregenna in Ref. [13] that a certain amount of decoherence can in fact produce useful properties in certain aspects of the walk. For certain structures, Kendon and Tregenna showed that the speed at which the walk goes toward a uniform distribution, which is of interest in some algorithmic applications, is increased by a certain amount of decoherence. Wong [14] investigates another kind of perturbation, in which a fault when shifting the walker can cause it to have a certain probability of staying put instead of shifting. He shows, under the assumption that this probability is uniform over the grid, that such a perturbation does not cause the walk to lose its ballistic behavior, but does in general cause the propagation speed of the walk to decrease.

In this thesis, we take inspiration from Kendon and Tregenna [13] and Wong [14] and study how faults in the implementation could induce different properties in the quantum walk. We model these faults, or perturbations, as potential barriers between grid positions, similar to that of Wong [14].

# Chapter 3

# Investigation

## 3.1 Problem

The aim of this thesis is to generalize the model of perturbing potential barriers between the discrete positions of the quantum walk from previous work [14] and to investigate how properties of the quantum walk are affected by the presence of these potential barriers. We compare these properties to those of the unperturbed quantum walk and the classical random walk. In particular, we are interested in the standard deviations of the position of the walks, as this is correlated to the propagation speed of the walker, and the general shape of the probability distributions arising from these walks.

Since the properties of the quantum walk on the line is often reflected in walks of other dimension and, as shown by Kempe [1], some unbiased walks on general graphs can be reduced to biased walks on the line, we restrict our scope to the one-dimensional, infinite grid i.e. the line.

## 3.2 Model

### Homogeneous Perturbing Potential

In the case of potential barriers between the positions, the walk will be perturbed during the shift procedure. See Fig. 3.1. The effect of this perturbation is to assign probabilities for tunneling to the new position and remaining at the current position. In Ref. [14] Wong considers the case of a constant homogeneous potential and models this by using a modified shift operator

$$S_p = \alpha S_f + \beta I, \tag{3.1}$$

where $S_f$ is the flip-flop operator to be defined below, $I$ is the identity operator and constants $\alpha$ and $\beta$ are complex numbers representing the tunneling and staying probability respectively. The flip-flop operator is defined as

$$S_f : \begin{cases} |\uparrow\rangle \otimes |i\rangle \xrightarrow{S_f} |\downarrow\rangle \otimes |i+1\rangle \\ |\downarrow\rangle \otimes |i\rangle \xrightarrow{S_f} |\uparrow\rangle \otimes |i-1\rangle \end{cases} . \tag{3.2}$$

From this definition, we see that the flip-flop operator is Hermitian, which leads to $S_p$ being unitary only under the conditions

$$|\alpha|^2 + |\beta|^2 = 1, \quad \alpha\beta^* + \alpha^*\beta = 0, \tag{3.3}$$

which is most easily satisfied by parameterizing the constants with a parameter $\phi \in [0, \frac{\pi}{2}]$ as $\alpha = \cos\phi$ and $\beta = i\sin\phi$. Note that the flip-flop operator is essentially the same as the ordinary shift operator $S$ except for the important difference that it also flips the coin state. Wong [14] gives several reasons to use the flip-flop operator instead of the standard shift operator $S$, such as it being faster in certain search algorithms [15]. Another reason is that the implementation in Ref. [12] uses this kind of shift operator, as the hyperfine states are in fact flipped after shifting. The two walks induced by the operators $U = S(C \otimes I_p)$ and $U_f = S_f(C \otimes I_p)$ are equivalent in the sense that they produce the same probability distributions, although not for the same basic initial states. The walk generated by $U$ from the initial state $|\psi\rangle = |\uparrow\rangle \otimes |0\rangle$ is the same as the one generated by $U_f$ from the initial state $|\psi\rangle = |\downarrow\rangle \otimes |0\rangle$.

## Arbitrary Perturbing Potential

We propose to expand this model to include non-homogeneous and time-varying potentials. To keep things simple, we continue to assume that the potentials consists of rectangular barriers between the positions of the walk. We can then expand Wong's model, Eq. (3.1), by making the constants depend on position and time, i.e. the number of steps taken, as well as the direction of the walker. Therefore our expanded potential takes on the form

$$S_{p,mod}\,|\psi_t\rangle = \begin{cases} (\alpha(i,t)S_f + \gamma_\uparrow(i,t)I)\,|\psi_t\rangle\,, & \text{if } |\psi_t\rangle = |\uparrow\rangle \otimes |i\rangle \\ (\beta(i,t)S_f + \gamma_\downarrow(i,t)I)\,|\psi_t\rangle\,, & \text{if } |\psi_t\rangle = |\downarrow\rangle \otimes |i\rangle \end{cases}, \tag{3.4}$$

where $\alpha$, $\beta$, $\gamma_\uparrow$ and $\gamma_\downarrow$ are position- and time-dependent complex constants. In order for the modified operator to be applicable on any kind of quantum walk, we demand the operator be unitary, which leads to the following conditions on the coefficients

$$\begin{aligned} |\alpha|^2 + |\gamma_\uparrow|^2 = 1, \quad \alpha\gamma_\uparrow^* + \gamma_\uparrow\alpha^* = 0, \\ |\beta|^2 + |\gamma_\downarrow|^2 = 1, \quad \beta\gamma_\downarrow^* + \gamma_\downarrow\beta^* = 0, \end{aligned} \tag{3.5}$$

which are easily satisfied by making $\alpha$ and $\beta$ real and $\gamma_\uparrow$ and $\gamma_\downarrow$ imaginary such that $\gamma_\uparrow = i\sqrt{1-\alpha^2}$ and $\gamma_\downarrow = i\sqrt{1-\beta^2}$, and where we can parametrize $\alpha$ and $\beta$ by $\phi \in [0, \frac{\pi}{2}]$, as done previously. Furthermore, by considering the potential as rectangular barriers between positions, we have symmetry conditions on the probability of going between two positions, namely $\alpha(i,t) = \beta(i+1,t)$ and $\beta(i,t) = \alpha(i-1,t)$, as shown in Fig. 3.1.

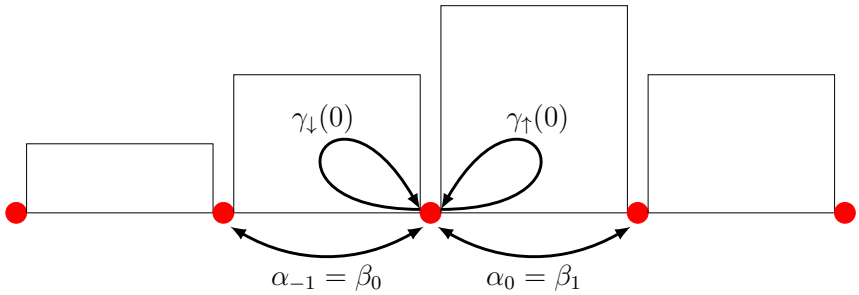


Figure 3.1: Illustration of potential on line with walking/staying coefficients.

## 3.3 Analytical Calculations

### The Discrete Fourier Transform

It is possible to obtain analytical expressions for the probability distribution of a walk on the line using Fourier analysis, as is done in Ref. [16] for the unperturbed walk on the infinite line. The reason being that the translational invariance of the walk makes analysis in the Fourier domain easier to manage. We will also perform this analysis, to test that our simulations are in agreement with the theory.
The coin state after $t$ steps at position $n$, $\psi(n,t) \in \mathbb{C}^2$, has a discrete Fourier transform

$$\Psi(k,t) = \sum_{n=-\infty}^{\infty} \psi(n,t)e^{ikn}, \tag{3.6}$$

where $k \in [-\pi, \pi]$. Conversely, the inverse Fourier transform is

$$\psi(n,t) = \frac{1}{2\pi}\int_{-\pi}^{\pi} \Psi(k,t)e^{-ikn}\mathrm{d}k. \tag{3.7}$$

The following derivation will start by finding a recurrence relation for a step in the walk at each position, which is easily analyzed in the Fourier domain.

### Fourier Analysis of Unperturbed Walk

Consider a position $n$ and a certain step of the walk, $t$, with some coin $C = \begin{bmatrix} a & b \\ c & d \end{bmatrix}$. After a step of the walk with the evolution operator $U_f = S_f(C \otimes I)$, the state at position $n$ can be written as

$$\psi(n,t+1) = \begin{pmatrix} c & d \\ 0 & 0 \end{pmatrix}\psi(n+1,t) + \begin{pmatrix} 0 & 0 \\ a & b \end{pmatrix}\psi(n-1,t).$$

Fourier transforming this recurrence relation, and using that $\sum_{n=-\infty}^{\infty}\psi(n+m,t)e^{ikn} = e^{-ikm}\sum_{n=-\infty}^{\infty}\psi(n,t)e^{ikn} = e^{-ikm}\Psi(k,t)$, it becomes

$$\Psi(k,t+1) = \begin{pmatrix} ce^{-ik} & de^{-ik} \\ ae^{ik} & be^{ik} \end{pmatrix}\Psi(k,t).$$

Thus a step in the walk is simply a multiplication by a certain matrix in the Fourier domain. Denoting $M = \begin{pmatrix} ce^{-ik} & de^{-ik} \\ ae^{ik} & be^{ik} \end{pmatrix}$, the recurrence relation implies that $\Psi(k,t) = M^t\Psi(k,0)$, i.e. that the walk in the Fourier domain consists of repeated application of the evolution matrix $M$. This can be computed efficiently by diagonalizing $M$. The eigenvalues are given as

$$\lambda = \frac{be^{ik} + ce^{-ik} \pm \sqrt{(ce^{-ik} - be^{ik})^2 + 4da}}{2}.$$

Examining the case of the Hadamard coin, $C = H$ gives $a = b = c = \frac{1}{\sqrt{2}}, d = \frac{-1}{\sqrt{2}}$, and

$$\lambda_\pm = \frac{e^{ik} + e^{-ik} \pm \sqrt{(e^{ik} - e^{-ik})^2 - 4}}{2\sqrt{2}} = \frac{\cos(k) \pm i\sqrt{\sin^2 k + 1}}{\sqrt{2}}.$$

By a change of variables to $\cos k = \sqrt{2}\cos(\omega_k)$ and $\sin\omega_k = \frac{\sqrt{\sin^2 k+1}}{\sqrt{2}}$, where $\omega_k \in [\frac{-\pi}{4}, \frac{\pi}{4}]$, the eigenvalues can be written as

$$\lambda_\pm = e^{\pm i\omega_k}.$$

Eigenvectors are found by solving

$$M\left|v_\pm\right\rangle = \lambda_\pm \left|v_\pm\right\rangle,$$

which has the solutions

$$\left|v_+\right\rangle = \frac{1}{A_+}\begin{pmatrix} 1 \\ 1 - \sqrt{2}e^{i(\omega_k + k)} \end{pmatrix}, \quad \left|v_-\right\rangle = \frac{1}{A_-}\begin{pmatrix} 1 \\ 1 - \sqrt{2}e^{i(k - \omega_k)} \end{pmatrix},$$

where $A_\pm$ are normalization factors, given by

$$A_\pm^2 = |v_\pm|^2 = 4 - 2\sqrt{2}\cos(k \pm \omega_k).$$

The walk in the Fourier domain can now be evaluated as

$$\Psi(k,t) = M^t\psi(k,0) = \lambda_+^t \left|v_+\right\rangle\left\langle v_+\right|\Psi(k,0) + \lambda_-^t \left|v_-\right\rangle\left\langle v_-\right|\Psi(k,0).$$

Considering the symmetric initial state, $\psi(0,0) = \frac{1}{\sqrt{2}}(1,i)^T$, i.e. the initial momentum wave-function $\Psi(k,0) = \frac{1}{\sqrt{2}}(1,i)^T$, the resulting state becomes

$$\begin{aligned} \Psi(k,t) = {} & e^{i\omega_k t}\frac{1 + i(1 - \sqrt{2}e^{-i(k+\omega_k)})}{4(\sqrt{2} - \cos(k + \omega_k))}\begin{pmatrix} 1 \\ 1 - \sqrt{2}e^{i(\omega_k + k)} \end{pmatrix} \\ & + e^{-i\omega_k t}\frac{1 + i(1 - \sqrt{2}e^{i(\omega_k - k)})}{4(\sqrt{2} - \cos(k - \omega_k))}\begin{pmatrix} 1 \\ 1 - \sqrt{2}e^{i(k - \omega_k)} \end{pmatrix}, \end{aligned} \tag{3.8}$$

after some simplification.

The desired solution is then obtained by applying the inverse Fourier transform according to Eq. (3.7), which can be evaluated numerically.

## Fourier Analysis with Homogeneous Potential

Similar analysis is now performed for a Homogeneous perturbing potential. We will follow the steps done by Wong [14], where the constants $\alpha$ and $\beta$ are introduced as coefficients in the modified step operator $S_p = \alpha S_f + \beta I$. Then for the walk with shift operator $S_p$ and coin operator $C = \begin{bmatrix} a & b \\ c & d \end{bmatrix}$ the recurrence relation between the steps in the walk is obtained as

$$\psi(n, t+1) = \alpha \begin{pmatrix} c & d \\ 0 & 0 \end{pmatrix} \psi(n+1, t) + \alpha \begin{pmatrix} 0 & 0 \\ a & b \end{pmatrix} \psi(n-1, t) + \beta \begin{pmatrix} a & b \\ c & d \end{pmatrix} \psi(n, t).$$

Investigating the walk with the Hadamard coin, the Fourier transform of this relation becomes

$$\begin{aligned} \Psi(k, t+1) &= \left( \frac{\alpha e^{-ik}}{\sqrt{2}} \begin{pmatrix} 1 & -1 \\ 0 & 0 \end{pmatrix} + \frac{\alpha e^{ik}}{\sqrt{2}} \begin{pmatrix} 0 & 0 \\ 1 & 1 \end{pmatrix} + \frac{\beta}{\sqrt{2}} \begin{pmatrix} 1 & 1 \\ 1 & -1 \end{pmatrix} \right) \Psi(k, t) \\ &= \frac{1}{\sqrt{2}} \begin{pmatrix} \alpha e^{-ik} + \beta & -\alpha e^{-ik} + \beta \\ \alpha e^{ik} + \beta & \alpha e^{ik} - \beta \end{pmatrix} \Psi(k, t) \\ &= M_h \Psi(k, t). \end{aligned}$$

Once again the recurrence relation is a multiplication with a matrix, meaning that $\Psi(k, t) = M_h^t \Psi(k, 0)$. To perform this multiplication efficiently, $M_h$ is diagonalized. Its eigenvalues $\lambda_\pm$ are found by solving the characteristic equation

$$\lambda^2 - \lambda \alpha \sqrt{2} \cos k + (\alpha^2 - \beta^2) = 0.$$

Given the conditions in Eq. (3.3) on $\alpha$ and $\beta$, and assuming $\alpha$ and $\beta$ are chosen as real and imaginary respectively, then $\alpha^2 - \beta^2 = 1$ and the solutions can be expressed as

$$\lambda_\pm = \frac{\alpha \cos k \pm i\sqrt{2 - \alpha \cos^2 k}}{\sqrt{2}},$$

and by introducing the new variable $\omega_k$ as $\cos \omega_k = \frac{\alpha \cos k}{\sqrt{2}}$ the eigenvalues become

$$\lambda_\pm = e^{\pm i \omega_k}.$$

The corresponding eigenvectors are obtained as

$$|v_+\rangle = \frac{1}{A_+} \begin{pmatrix} 1 \\ \frac{\alpha + \beta e^{ik} - \sqrt{2} e^{i(\omega_k + k)}}{\alpha - \beta e^{ik}} \end{pmatrix}, \quad |v_-\rangle = \frac{1}{A_-} \begin{pmatrix} 1 \\ \frac{\alpha + \beta e^{ik} - \sqrt{2} e^{i(-\omega_k + k)}}{\alpha - \beta e^{ik}} \end{pmatrix},$$

with normalization factors $A_\pm$ given by

$$\langle v_\pm | v_\pm \rangle = 1 \implies A_\pm^2 = \frac{4 - 2\sqrt{2}\alpha \cos(k \pm \omega_k) \pm i 2\sqrt{2}\beta \sin(\omega_k)}{1 - 2i\alpha\beta \sin k},$$

where we again have used the conditions (3.3) for $\alpha$ and $\beta$.
Now the final momentum wave vector can be obtained according to

$$\Psi(k, t) = M_h^t \psi(k, 0) = \lambda_+^t |v_+\rangle \langle v_+| \Psi(k, 0) + \lambda_-^t |v_-\rangle \langle v_-| \Psi(k, 0).$$

Considering the initial momentum wave vector $\Psi = \frac{1}{\sqrt{2}}(1, i)^T$, which corresponds to the same initial state, the resulting vector becomes

$$\begin{aligned}\Psi(k,t) = e^{i\omega_k t}\frac{\left(1+\frac{i(\alpha-\beta e^{-ik}-\sqrt{2}e^{-i(k+\omega_k)})}{\alpha+\beta e^{-ik}}\right)(1-2i\alpha\beta\sin k)}{4(\sqrt{2}-\alpha\cos(k+\omega_k)+i\beta\sin\omega_k)}\begin{pmatrix}1\\ \frac{\alpha+\beta e^{ik}-\sqrt{2}e^{i(\omega_k+k)}}{\alpha-\beta e^{ik}}\end{pmatrix}\\ + e^{-i\omega_k t}\frac{\left(1+\frac{i\left(\alpha-\beta e^{-ik}-\sqrt{2}e^{i(\omega_k-k)}\right)}{\alpha+\beta e^{-ik}}\right)(1-2i\alpha\beta\sin k)}{4(\sqrt{2}-\alpha\cos(k-\omega_k)-i\beta\sin\omega_k)}\begin{pmatrix}1\\ \frac{\alpha+\beta e^{ik}-\sqrt{2}e^{i(-\omega_k+k)}}{\alpha-\beta e^{ik}}\end{pmatrix}.\end{aligned} \tag{3.9}$$

We note that setting $\alpha = 1$ and $\beta = 0$ gives the same expression as in Eq. (3.8), which is to be expected since these values reduce the modified $S_p$ to the normal flip-flop shift operator $S_f$. The corresponding coin state is now calculated by the inverse Fourier transform according to Eq. (3.7), and evaluated numerically.

### Walk with Arbitrary Potential Barriers

While one would want to analytically research the walk with an arbitrary potential, the fact that the potential is arbitrary introduces difficulties in the Fourier analysis. The convenience of the Fourier analysis, as stated, lies in that the walk is translationally invariant. By introducing arbitrary potentials into the walk, the walk could lose this property, and we are forced to Fourier transform not only $\psi$, but products of $\psi$, $\alpha$, $\beta$ and $\gamma$ coefficients. This makes the analysis of the recurrence formula too difficult to cover in this paper.

## 3.4 Numerical Analysis and Simulations

The inverse Fourier transform of the analytical results from the last section are evaluated numerically by using MATLAB and its built in numerical integration functions.

As for the cases where we do not solve for the probability distribution of the walk analytically, the walk is instead simulated numerically. In this section, we briefly present the implementation of the quantum walk simulation, written using the NumPy package in Python.

For a walk with $N$ steps, the state space of the walker can be represented by a list of length $2N + 1$, holding the coin state vector for each position. The probability of being in a position is then given by the square of the Euclidean norm of the coin state vector at the corresponding position in the list.

Given this structure, simulating the walk consist of applying the relevant shift- and coin operators repeatedly. As the coin operator corresponds to multiplication of the coin state with a simple two by two matrix, it is trivial to implement. The shift operator involves moving the coin state vector components to adjacent list elements, which is done differently depending on the shift operator in use. But for the most involved case of the modified shift operator with a potential, the $|\uparrow\rangle$ component of the coin state is multiplied by the corresponding staying coefficient and a product of it and the corresponding walking coefficient is added to the $|\downarrow\rangle$ component to the right. The same is done for the $|\downarrow\rangle$ component, to the left and with corresponding coefficients. But to do this sequentially over all positions, the modified coin states are saved separately until all positions have

been processed. After this is done for all positions and the coin states are updated, the shift operator has been successfully applied.

The simulation then consists of: Creating the list, initializing the walk by specifying the coin state at the start position and specifying the potentials, and then applying the coin operator followed by the shift operator a specified number of times. Computing the norm of the coin state at every position then gives the probability distribution of the walker.

## 3.5 Results

First we examine the unperturbed walk with the evolution operator $U_f = S_f(C \otimes I)$ and compare it to the probability distribution of the classical walk. We also compare our simulation of the walk to the numerical evaluation of analytical expression obtained from the Fourier analysis in sections 3.3 and 3.3. The residual between the simulation and the analytical result is seen in Fig. 3.3.

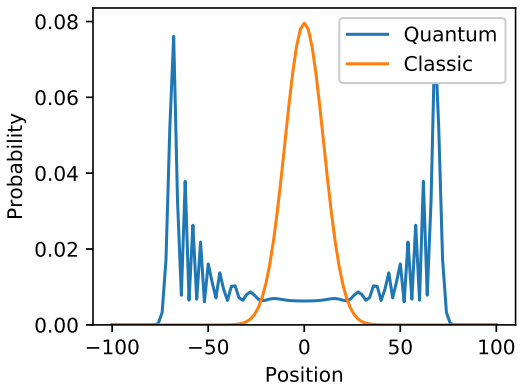


Figure 3.2: Simulation of 100 step random walk plotted against 100 step quantum random walk with odd-valued positions ignored. Quantum initial state was $|\psi_0\rangle = \frac{1}{\sqrt{2}}(|\uparrow\rangle + i\,|\downarrow\rangle) \otimes |0\rangle$.

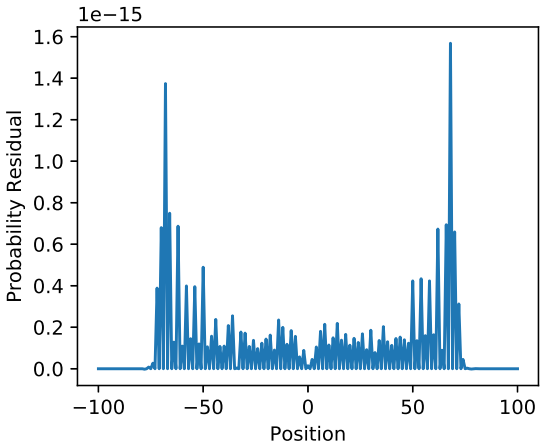


Figure 3.3: Residual between numerical evaluation of analytical expression for 100 step random walk and simulation. Initial state was $|\psi_0\rangle = \frac{1}{\sqrt{2}}(|\uparrow\rangle + i\,|\downarrow\rangle) \otimes |0\rangle$.

In the next figure, Fig. 3.4, we show the trends of the standard deviation as a function of the number of steps for the unperturbed quantum and classical walk. We observe that the standard deviation of the quantum distribution is indeed linear after a few steps, as seen by the slope of the quantum line having slope 1 after step 3. And as expected, the classical distribution seems to follow a $\sqrt{t}$ trend, by the slope of 0.5 for the classical line.

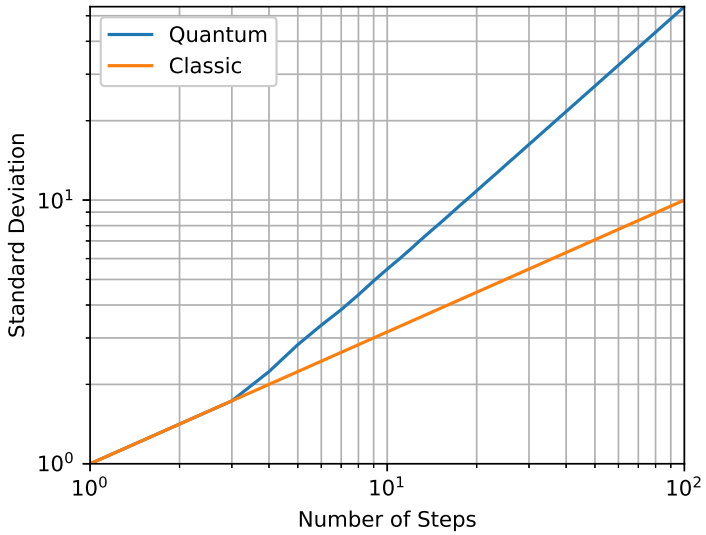


Figure 3.4: Loglog plot of standard deviation of the unperturbed quantum walk against that of the classical walk, as a function of the number of steps. Quantum initial state was $|\psi_0\rangle = \frac{1}{\sqrt{2}}(|\uparrow\rangle + i\,|\downarrow\rangle) \otimes |0\rangle$. The quantum line is measured to have slope 1 after step 3 and the classical line has slope 0.5.

Below we examine the distribution obtained after having a homogeneous perturbing barrier distribution of strength $\phi = 0.8$, shown in Fig. 3.5, as done in the paper by Wong [14]. We then compare with the analytical result by looking at the residual between simulation and analytical probability distributions.

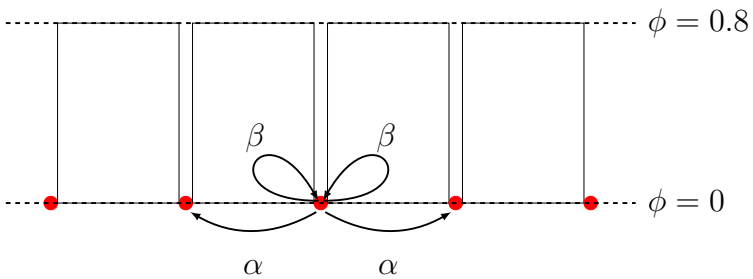


Figure 3.5: Illustration of homogeneous perturbing potential with strength $\phi = 0.8$ with parameters $\alpha$ and $\beta$ in the model described by Wong.

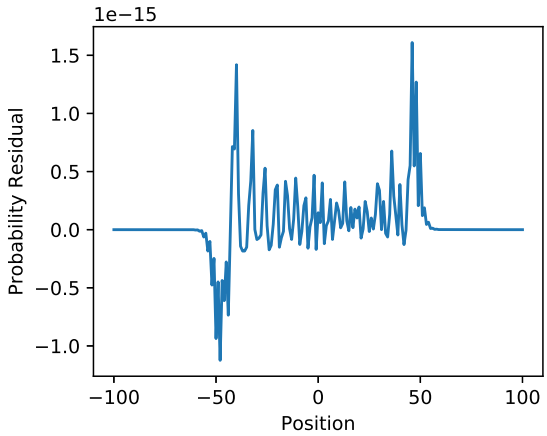


Figure 3.6: Residual between simulations and numerical evaluation of analytical expressions obtained for the 100 step walk with a homogeneous potential with $\alpha = 0.70$ and $\beta = 0.72i$, i.e. strength $\phi = 0.8$ (as seen in Fig. 3.5). Initial state was $|\psi_0\rangle = \frac{1}{\sqrt{2}}(|\uparrow\rangle + i\,|\downarrow\rangle) \otimes |0\rangle$.

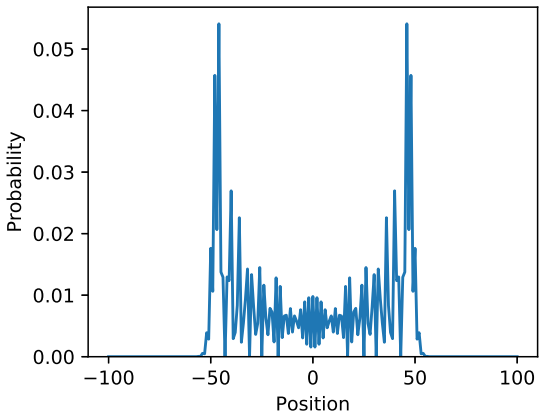


Figure 3.7: Simulation of a 100 step quantum random walk with homogeneous perturbing potential with $\alpha = 0.70$ and $\beta = 0.72i$, i.e. strength $\phi = 0.8$ (as seen in Fig. 3.5). Initial state was $|\psi_0\rangle = \frac{1}{\sqrt{2}}(|\uparrow\rangle + i\,|\downarrow\rangle) \otimes |0\rangle$.

For this potential, we also show the standard deviation as a function of the number of steps and compare it with the unperturbed quantum walk. In the loglog plot, Fig. 3.8, it can be observed that the perturbed case also follow a linear trend and that the propagation speed is lower than in the unperturbed case. From this, we investigate the linear slope of the standard deviation, as a function of the potential strength $\phi \in [0, \frac{\pi}{2}]$, where $\phi = \frac{\pi}{2}$ is the case when the walker is completely blocked from taking a step, and $\phi = 0$ is the unperturbed walk resulting in Fig. 3.9.

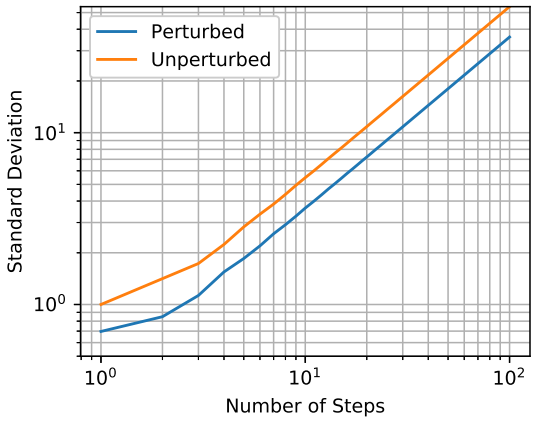


Figure 3.8: Loglog plot of standard deviation of perturbed quantum walk, with homogeneous potential, against that of the unperturbed quantum walk, as a function of the number of steps. Initial state was $|\psi_0\rangle = \frac{1}{\sqrt{2}}(|\uparrow\rangle + i\,|\downarrow\rangle) \otimes |0\rangle$.

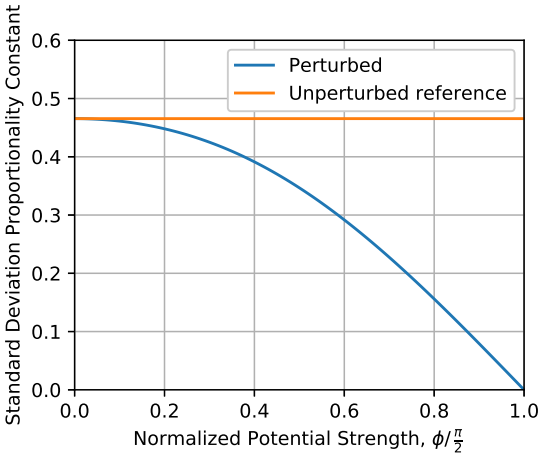


Figure 3.9: Standard deviation linear slope of perturbed quantum walk as a function of normalized potential strength $\phi$. Calculated from simulation of a 100 step walk with initial state $|\psi_0\rangle = \frac{1}{\sqrt{2}}(|\uparrow\rangle + i\,|\downarrow\rangle) \otimes |0\rangle$.

Now we examine the effect of a special potential, a potential localized around the start position with width of 2 steps, meaning the potential exists between position -1, 0 and 1, as seen in Fig. 3.10.

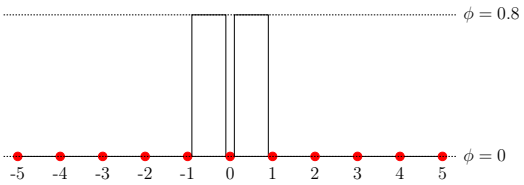


Figure 3.10: Illustrative figure of localized perturbing potential around the starting position. The barriers have a strength of $\phi = 0.8$ where non-zero.

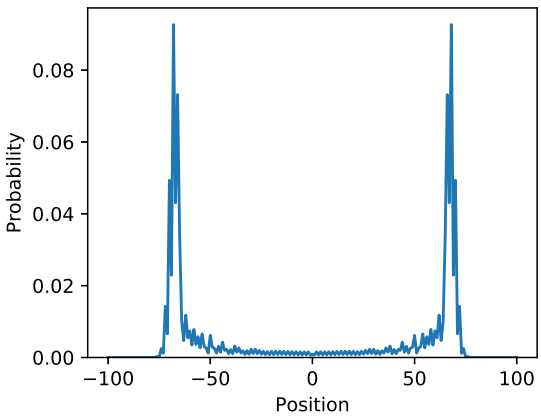


Figure 3.11: Simulation of a 100 step quantum random walk with non-homogeneous perturbing potential, localized around the start position. Initial state was $|\psi_0\rangle = \frac{1}{\sqrt{2}}(|\uparrow\rangle + i\,|\downarrow\rangle) \otimes |0\rangle$

This potential seems to have eliminated much of the probability around the starting

position, concentrating the probability in the two propagating spikes. In the standard deviation plot (Fig. 3.12), we also see that the potential increases the overall propagation of the distribution, while keeping an approximate linear trend for most steps. We then investigate the effect of this potential on the standard deviation as a function of the potential strength, which is seen in Fig. 3.13. This kind of potential was also examined with different widths, and we also tested turning the potential off after a certain number of steps. Simulations showed that the standard deviation increase quickly diminished for increasing width of the localized potential. On the other hand, it was also shown that turning the potential off after a certain number of steps did not diminish its effect on the probability distribution.

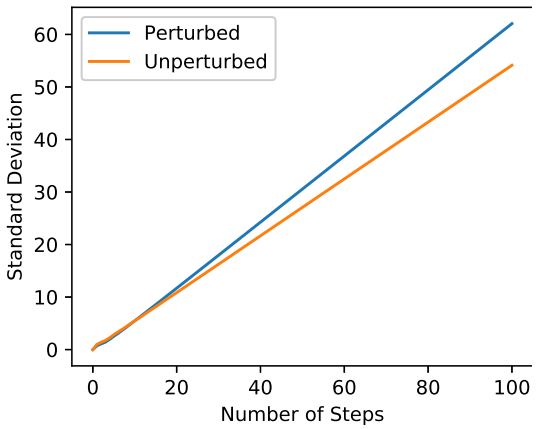


Figure 3.12: Standard deviation of perturbed quantum walk, with localized potential, against that of the unperturbed quantum walk, as a function of the number of steps. Initial state was $|\psi_0\rangle = \frac{1}{\sqrt{2}}(|\uparrow\rangle + i\,|\downarrow\rangle) \otimes |0\rangle$.

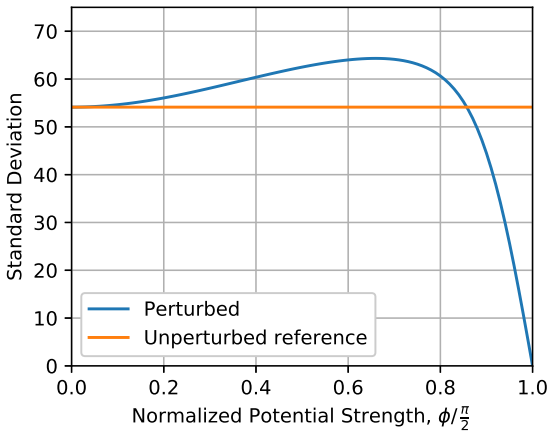


Figure 3.13: Standard deviation measured as function of potential strength $\phi$, for a potential barrier localized at the start position with a width of 2. Measured after simulation of perturbed 100 step walk with initial state $|\psi_0\rangle = \frac{1}{\sqrt{2}}(|\uparrow\rangle + i\,|\downarrow\rangle) \otimes |0\rangle$.

We now examine a potential where we choose the potential strengths randomly. We do this by for each barrier choosing a value $\phi$ from a uniform probability distribution on the interval $[0, k]$, where $k$ is some constant less than $\frac{\pi}{2}$and simulate the walk with this potential. Since each simulation is random, no two potentials are the same for this case. To investigate the average effect of the distribution, we hence simulate 100 walks of 100 steps with such a random potential and take the average of the resulting distributions. The result is as seen in Fig. 3.14 for $k = 0.5$ and in Fig. 3.15 for $k = 0.8$.

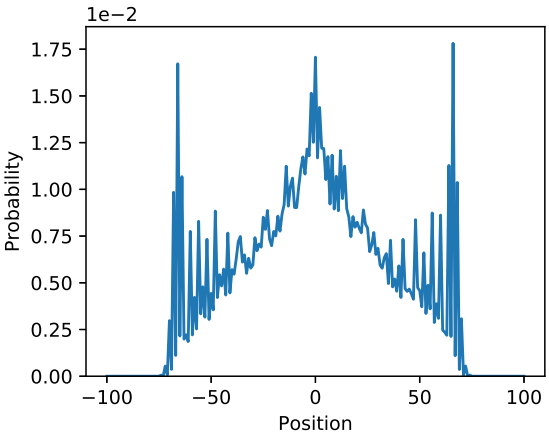


Figure 3.14: Average probability distribution of 100 simulated 100 step walks with uniformly random potential with strength between 0 and $k = 0.5$. Initial state was $|\psi_0\rangle = \frac{1}{\sqrt{2}}(|\uparrow\rangle + i\,|\downarrow\rangle) \otimes |0\rangle$.

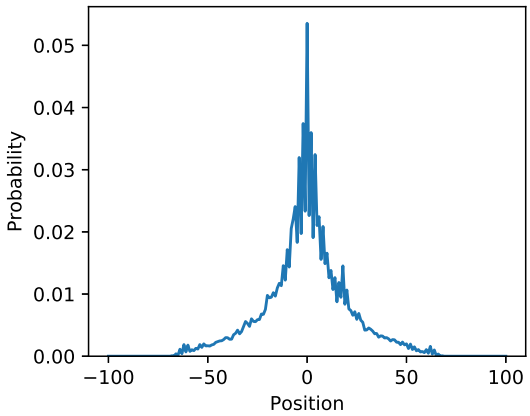


Figure 3.15: Average probability distribution of 100 simulated 100 step walks with uniformly random potential with strength between 0 and $k = 0.8$. Initial state was $|\psi_0\rangle = \frac{1}{\sqrt{2}}(|\uparrow\rangle + i\,|\downarrow\rangle) \otimes |0\rangle$.

## 3.6 Discussion

Our results regarding quantum walks without potentials, both the numerical simulation performed for different initial states and the analytical solution of the symmetric initial state $\psi_0 = \frac{1}{\sqrt{2}}(|\uparrow\rangle + i\,|\downarrow\rangle) \otimes |0\rangle$, are in good agreement with previously stated results of the quantum walk being ballistic, with a standard deviation $\sim t$, in contrast to the diffusive classical walk with standard deviation $\sim \sqrt{t}$. We can also confirm that the walk with the flip-flop operator $S_f$ produces the same probability distribution for the symmetric walk as the walk with the ordinary shift operator $S$, as was stated by Wong [14].

To make sure that the implementation of the quantum walk as described in Section 3.4 was correct, the simulated walk was compared against short walks calculated by hand, as done in Section 2.2 and the results were in good agreement. To check that all operators involved were indeed unitary, the probability of the walker being found *somewhere* on the grid after measurement was always calculated and found equal to 1.

We further tested the implementation by comparing it to the analytical solutions in the cases with $|\psi_0\rangle = \frac{1}{\sqrt{2}}(|\uparrow\rangle + i\,|\downarrow\rangle) \otimes |0\rangle$ and as seen in the residuals in Fig. 3.3 and Fig. 3.6, the error is of the order $10^{-15}$. Compared to the measured probabilities of the order $10^{-2}$, the error is negligible and definitely in the range of numerical error when computing or integrating. For the arbitrary perturbing potential we did not have the option of comparing to any analytical solution, nor compare to previous work. Instead we checked some limiting cases where we intuitively knew how the walk would behave, for example that the walk comes to a halt where the potential strength is $\phi = \frac{\pi}{2}$, corresponding to a shift operator $S_f = iI$.

In accordance with how Wong [14] shows that the position of the peaks in the quantum distribution moves linearly, we find that the standard deviation of the walk remains

linear in $t$ as we introduce a potential constant in time and space, regardless of strength. Further, after having quantified the dependence of the standard deviation on the potential strength, we find, as expected, that the standard deviation decreases continuously as the potential strength increases. This dependence could possibly be used to identify perturbations of the potential in implementations of the quantum walk by noting the propagation speed of the walk and comparing to Fig. 3.9.

In introducing a highly localized potential around the starting position of the walker, the probability distribution, shown in Fig. 3.11, gives a higher standard deviation than the walk without any potential. This effect is present for any potential strength $0.10\frac{\pi}{2} \lesssim \phi \lesssim 0.85\frac{\pi}{2}$, as seen by the trend of the standard deviation in Fig. 3.13. Comparing Fig. 3.10 and Fig. 3.2, it can be seen that the potential does not increase the maximum propagation distance of the distribution. It instead focuses probability around the starting position onto the outermost peaks, basically making the walk into two fairly localized particle waves traveling outward from the starting position. Overall, it increases the ballistic nature of the quantum walk. Further, we found that this effect remained, despite setting the potential strength to 0 after a few steps. The effect was diminished by increasing the width of the potential resulting in a smaller increase in standard deviation. Therefore, if one were to implement such a potential in order to obtain this characteristic of the walk, it would be necessary to control the width of the potential to a certain degree, but it would not be necessary to perturb the walk at every step. This is assuming turning the perturbing potential off does not introduce any other effect that might affect the walk differently.

In contrast to the localized potential, the general effect of having a uniformly distributed random potential seems to be localization of the walker around the starting position. The distributions of each walk evolves according to the particular realization of the random potential. Because of that, the average distribution was investigated instead, in order to find more general behavior during these walks. It was found that the probability around the starting position increases as a function of the maximum potential strength. Simulating for different maximum strengths, we found that the average distribution gradually converges to an exponentially localized state, as can be seen in Fig. 3.14 and Fig. 3.15. This is quite similar to the problem of Anderson localization where the propagation of a wave is largely prevented by the disorder of the medium. This shows that the walker might be affected by disorder in the grid, the same way as a wave traveling through a disordered medium. As implementations of the quantum walk will realistically have some kind of imperfections, likely to be random in nature, some disorder could be present and cause the walker to become localized to a certain degree.

# Chapter 4

# Summary and Conclusions

In this thesis, we simulated the discrete quantum walk in order to examine its properties on the line and compared them to that of the classic random walk. We investigated perturbations in the shift sequence causing the walker to have a probability of not moving and modeled this as potential barriers between the positions of the grid, inspired by previous work by Wong [14]. We studied different kinds of potential barrier distributions and their effects on the probability distribution and standard deviation of the quantum walk.

Homogeneous potential barriers could be seen to have the effect of decreasing the propagation speed of the walk, while retaining its ballistic properties. A localized potential could on the other hand increase the ballistic property of the walk, focusing most of the probability onto two fairly localized peaks moving outward from the starting position and increasing the standard distribution. For a uniformly distributed random potential, the disorder in the random potential caused localization at the starting position, similar to that of Anderson localization.

In conclusion, we have found that introducing potential barriers can result in many different new behaviors. While we did find interesting properties of the quantum walk by introducing potentials, we did not come close to exhausting the supply of relevant potentials to study, and it remains to see to exactly what extent one can influence the walk. One open question would be if there exists a potential distribution with effects similar to the localized potential, but that is also able to make the probability maximum of the walk propagate further.

There are also many situations we did not consider in this thesis. We have for example only briefly considered time dependence for potentials and we have not at all concerned ourselves with potentials of non-rectangular shape. It might also be interesting to treat the case when other perturbations to the implementation of the walk, such as decoherence, are present along with potentials.

# Acknowledgements

We would like to express our deepest gratitude to our supervisor Professor Mats Wallin, who gave a lot of his time to discuss this subject with us and provided us with invaluable guidance throughout the course of this thesis.

We also want to thank Malin Atterving and Charles Gilljam for giving us useful feedback during the writing of this thesis.

# Bibliography


[1] Kempe J. Quantum random walks - an introductory overview. *Contemporary Physics*, Vol. 44 (4), p. 307-327, 2003, quant-ph/0303081.

[2] Shor P W. Algorithms for quantum computation: Discrete logarithms and factoring. 35th *Annual Symposium on Foundations of Computer Science* 1994 (Los Alamitos, CA: IEEE Computer Society Press), p. 124.

[3] Shenvi N, Kempe J and Whaley K B. Quantum random-walk search algorithm. *Physical Review A*, vol. 67, 052307, 2003.

[4] Schöning U. A Probabilistic Algorithm for k-SAT and Constraint Satisfaction Problems. 40th *Annual Symposium on Foundations of Computer Science* 1999 (Los Alamitos, CA: IEEE Computer Society Press) p. 17-9.

[5] Kempe J. Quantum Random Walks Hit Exponentially Faster. *Probability Theory and Related Fields*, Vol. 133(2), p. 215-235 (2005), quant-ph/0205083.

[6] Reitzner D, Nagaj D, Bužek V. Quantum Walks. *Acta Physica Slovaca 61*, No.6, 603-725 (2011), quant-ph/1207.7283.

[7] Halmos P. Spaces. In *Finite Dimensional Vector Spaces* 2nd edition, Springer-Verlag New York, 1958.

[8] Tregenna B, Flanagan W, Maile R and Kendon V. Controlling discrete quantum walks: coins and initial states. *New Journal of Physics* 5 (2003) 83.1-83.19.

[9] Travaglione B C, Milburn G J. Implementing the quantum random walk. *Physical Review A*, 65:032310, 2002.

[10] Sanders B C, Bartlett S D, Tregenna B, and Knight P L. *Quantum quincunx in cavity quantum electrodynamics*, 2002. quant-ph/0207028.

[11] Dür W, Raussendorf R, Kendon V M, and Briegel H J. Quantum random walks in optical lattices. *Physical Review A*, 66:052319, 2002.

[12] Karski M, et al. *Quantum Walk in Position Space with Single Optically Trapped Atoms*, 2009, quant-ph/0907.1565.

[13] Kendon V, Tregenna B. Decoherence can be useful in quantum walks. *Physical Review A* 67 042315 2003, quant-ph/0209005.

[14] Wong T G. Quantum walk on the line through potential barriers. *Quantum Information Processing* 15(2) p. 675-688, quant-ph/1503.06605.

[15] Ambainis A, Kempe J, Rivosh A. Coins make quantum walks faster. In: *Proceedings of the 16th Annual ACM-SIAM Symposium on Discrete Algorithms*, SODA '05, pp. 1099-1108. SIAM, Philadelphia, PA, USA (2005).

[16] Portugal R. *Quantum Walks and Search Algorithms*, London: Springer New York, 2013.